https://doi.org/10.1016/j.jes.2021.01.018

Measurement of heterogeneous uptake of NO_2 on inorganic particles, sea water and urban grime

Chuan Yu[1,2], Zhe Wang[3,*], Qingxin Ma[4], Likun Xue[1], Christian George[5], and Tao Wang[2,*]

1. Environment Research Institute, Shandong University, Qingdao 266237, China
2. Department of Civil and Environmental Engineering, The Hong Kong Polytechnic University, Hong Kong 999077, China
3. Division of Environment and Sustainability, The Hong Kong University of Science and Technology, Hong Kong 999077, China
4. Research Center for Eco-Environmental Sciences, Chinese Academy of Sciences, Beijing 100085, China
5. Univ Lyon, Université Claude Bernard Lyon 1, Centre national de la recherche scientifique (CNRS), Institut de recherches sur la catalyse et l'environnement de Lyon (IRCELYON), Villeurbanne F-69626, France

Abstract: Heterogeneous reactions of NO_2 on different surfaces play an important role in atmospheric NO_x removal and HONO formation, having profound impacts on photochemistry in polluted urban areas. Previous studies have suggested that the NO_2 uptake on the ground or aerosol surfaces could be a dominant source for elevated HONO during the daytime. However, the uptake behavior of NO_2 varies with different surfaces, and different uptake coefficients were used or derived in different studies. To obtain a more holistic picture of heterogeneous NO_2 uptake on different surfaces, a series of laboratory experiments using different flow tube reactors was conducted, and the NO_2 uptake coefficients (γ) were determined on inorganic particles, sea water and urban grime. The results showed that heterogeneous reactions on those surfaces were generally weak in dark conditions, with the measured γ varied from $<10^{-8}$ to 3.2×10^{-7} under different humidity. A photo-enhanced uptake of NO_2 on urban grime was observed, with the obvious formation of HONO and NO from the heterogeneous reaction. The photo-enhanced γ was measured to be 1.9×10^{-6} at 5% relative humidity (RH) and 5.8×10^{-6} at 70% RH on urban grime, showing a positive RH dependence for both NO_2 uptake and HONO formation. The results demonstrate an important role of urban grime in the daytime NO_2-to-

HONO conversion, and could be helpful to explain the unknown daytime HONO source in the polluted urban area.

Keywords:

NO_2 uptake

HONO source

Heterogeneous uptake coefficient

Urban grime

---

* Corresponding authors. E-mails: z.wang@ust.hk (Zhe Wang), cetwang@polyu.edu.hk (Tao Wang)

Introduction

The heterogeneous reaction of NO_2 on different surfaces acts as an important NO_x sink and a major source of nitrous acid (HONO), thus affecting the atmospheric nitrogen cycle and photochemistry (Finlayson-Pitts et al., 2003). Several previous laboratory studies have measured the heterogeneous uptake of NO_2 on inorganic particles, such as SiO_2 (Underwood et al., 2001; Ndour et al., 2009), Al_2O_3 (Underwood et al., 1999; Borensen et al., 2000), $CaCO_3$ (Li et al., 2010b) and minieral dust (Zhou et al., 2015), but the reactivity of NO_2 on inorganic particles (expressed as an uptake coefficient, γ) is usually low (γ lies in the range from $<10^{-8}$ to 10^{-7}). However, some studies reported much higher γ on NaCl particles, around 10^{-4} (Abbatt and Waschewsky, 1998; Harrison et al., 1998). The discrepancies need to be revisited because previous experiments were conducted with different techniques and conditions far from the ambient, such as high reactant concentrations or in vacuum systems (e.g., Underwood et al., 1999; Börensen et al., 2000; Guan et al., 2014).

Enhanced reactivity of NO_2 was found when irradiation was involved in the heterogeneous process. For example, the photo-enhanced uptake of NO_2 have been found on polycyclic aromatic hydrocarbons (PAHs) (George et al., 2005; Brigante et al., 2008; Ammar et al., 2010; Cazoir et al., 2014), humic acid (HA) (e.g., Stemmler et al., 2006, 2007; Han et al., 2016), soot (Monge et al., 2010; Guan et al., 2017) and mineral dust (Ndour et al., 2008, 2009). The photo-enhanced γ is usually within 10^{-7}-10^{-6}, larger than those on inorganic particles at dark by one or two orders of magnitude. Moreover, enhanced HONO formation was also often observed

together with the photo-enhanced uptake of NO_2 (e.g., George et al., 2005; Brigante et al., 2008; Ammar et al., 2010; Cazoir et al., 2014; Stemmler et al., 2006, 2007; Monge et al., 2010).

HONO could act as an important source of hydroxyl radical (OH) through photolysis and therefore plays an important role in the oxidation capacity of the atmosphere. The gas-phase reaction of NO and OH and nocturnal heterogeneous reaction of NO_2 on surfaces have been recognized as the major HONO sources at daytime and nighttime, respectively (e.g., Kleffmann, 2007; Finlayson-Pitts et al., 2003). A recent study at a coastal site in Hong Kong has observed that the NO_2-to-HONO conversion rate in the air masses passing over the sea was almost 3 times larger than that in the land air masses, suggesting that the air-sea interaction at the sea surface could be a source of HONO (Zha et al., 2014). Some studies also revealed significant unknown daytime sources of HONO that cannot be explained by the traditional gas-phase oxidation process (Su et al., 2011), and several potential daytime sources or mechanism have been proposed, including traffic emissions (Kurtenbach et al., 2001; Liang et al., 2017), photo-enhanced heterogeneous reaction of NO_2 on surfaces containing humic acid, PAHs and soot (e.g., Stemmler et al., 2006; George et al., 2005; Monge et al., 2010), photolysis of nitrate (e.g., Nanayakkara et. al., 2014; Ye et al., 2016; Baergen and Donaldson, 2013; Ye et al., 2017) and nitric acid (Zhou et al., 2003; Laufs et al., 2016), etc.

In the urban area, particles and urban surfaces provide a large surface area for the heterogeneous reactions of trace gases. A model study predicted that in the highly urbanized area, the surface area provided by the ground surface could be 3 times larger than the atmospheric aerosol surface, and could be more important for the heterogeneous reaction of NO_2 in urban areas (Zhang et al., 2016). Furthermore, urban surfaces such as buildings and roads are usually covered with a film of a complex mixture of organic and inorganic materials, which are called urban grime (Baergen et al. 2015; Lam et al., 2005; Liu et al., 2003; Butt et al., 2004; Wang et al., 2012). A recent study has reported a photo-enhanced uptake of NO_2 and HONO production on real urban grime, with γ of $(1.1\text{-}5.8) \times 10^{-6}$ at RH range of 0% - 90% (Liu et al. 2019). As the physical and chemical properties of urban grime vary with locations (Baergen et al. 2015; Lam et al., 2005; Liu et al., 2003; Butt et al., 2004), the heterogeneous behavior of NO_2 on more urban grime under different conditions should be investigated (Liu et al. 2019), in order to better quantify the roles of heterogeneous reactions on urban grime in HONO production and urban air quality, especially for highly urbanized environment with more NO_x emission and building surfaces.

In this study, to enrich the present understanding of NO_2 heterogeneous reactivity and to explore the unknown source of HONO, we conducted a series of laboratory experiments on

different surfaces. We revisited the heterogeneous uptake of NO_2 on SiO_2, Al_2O_3, $CaCO_3$, NaCl, and $(NH_4)_2SO_4$ particle surface by a coated-wall flow tube, and measured its uptake on NaCl solution and sea water surface using a wetted-wall flow tube. We also investigate the NO_2 heterogeneous process and HONO production on urban grimes collected in Hong Kong with high building density and compact urban setting.

1 Materials and methods

1.1 Coated wall flow tube

A horizontal cylindrical coated-wall flow tube was used to study the NO_2 uptake on solid particles (**Fig. 1a**), and similar apparatus and techniques have been employed and described in many studies (Han et al., 2013; Liu et al., 2015; Ma et al., 2017). The flow tube was made of quartz glass with a length of 34 cm and an inner diameter of 1.6 cm. Powder sample was dissolved in 20.0 mL of deionized water (for MgO, SiO_2, Al_2O_3, and $CaCO_3$) or ethanol (for NaCl and $(NH_4)_2SO_4$) and then was dripped into a quartz tube (20.0 cm length, 1.1 cm inner diameter) and dried for 12 hours in an oven at 373 K. SiO_2 (99.9%), Al_2O_3 (99.9%), $CaCO_3$ (99.9%), NaCl (99.9%), $(NH_4)_2SO_4$ (99.9%) and ethanol (99.9%) were purchased from Sigma-Aldrich. The specific surface area was measured by nitrogen Brunauer-Emmett-Teller (BET) physisorption (Autosorb-1-C, Quantachrome, USA) and was 135.6 m^2/g for MgO, 4.2 m^2/g for SiO_2, 12 m^2/g for Al_2O_3, 0.6 m^2/g for $CaCO_3$, 0.22 m^2/g for NaCl, and 0.16 m^2/g for $(NH_4)_2SO_4$, respectively. Experiments were carried out at 295 K by thermostatic circulation of water through the outer jacket of the flow tube and the flow tube was covered to shield from the light during the experiments. Zero air was introduced in the flow tube as carrier gas at a flow rate of 0.9 L/min, ensuring a laminar regime. The RH of the carrier gas was adjusted by a water bubbler. NO_2 (10 ppmv in N_2; 99%; Arkonic) was introduced in the flow tube via a movable injector (with an inner diameter of 0.3 cm) and the NO_2 concentration in the total flow was 100 ppbv. At the exit of the flow tube, NO concentration, NO_2 concentration and RH were measured.

1.2 Wetted wall flow tube

A wetted wall flow tube system was developed following the design of Behnke et al. (1997) and Gutzwiller et al. (2002). The vertical flow tube was made of glass with a length of 120 cm and an inner diameter of 0.8 cm (**Fig. 1b**). Experiments were carried out at 295 K by thermostatic circulation of water through the outer jacket of the flow tube and the flow tube was covered to shield from the light during the experiments. NaCl solution (3.5 wt.%) was prepared by NaCl (99.9%; Sigma-Aldrich) and deionized water. Sea water was collected at Hok

Tsui, Hong Kong in July 30, 2017. Reagent (NaCl solution or sea water) was pumped in at the top of the wetted wall flow tube by a peristaltic pump at a flow rate of 3 mL/min. Using an annular reservoir dispenser system, the reagent flowed down uniformly on the inner wall of the flow tube and was pumped out at the bottom of the flow tube. A dry mixture of NO_2 and zero air (NO_2 concentration of 300 ppbv) was introduced in the flow tube at a flow rate of 0.4 L/min, ensuring a laminar regime. Then after contact with the reagent, the gas exited from a Teflon moveable extractor and diluted by dry zero air at a flow rate of 1.7 L/min. RH at the exit of the wetted wall flow tube was measured to be around 26%. NO, NO_2 and HONO concentrations in the outflow were monitored.

1.3 Teflon box reactor

A PFA box reactor (inner size of 25 cm × 15 cm × 5 cm, with a 22.5 cm × 12.5 cm FEP window on the top) was used to study the uptake coefficient of NO_2 on urban grime (**Fig. 1c**). The box was covered to shield from the light in the dark experiments or illuminated by an 18 W UV-visible light (Arcadia Products plc., UK) in the irradiation experiments. A fan outside the reactor was used for cooling the UV-visible light, and the experiments were performed at room temperature around 295 K. Before the experiment, the spectral irradiance inside the reactor was measured by a Spectro-Radiometer (Specbos 1211UV, JETI Technische Instrumente GmbH., Germany), and had a continuous emission in the range of 280-780 nm and a dominant wavelength <450nm (**Fig. 1d**). The total irradiance was 2.1 W/m^2, and was 0.53 W/m^2 under near-UV range, which was similar to the UV irradiances of 0.69 W/m^2 (Ndour et al., 2008) and 0.72 W/m^2 (Nanayakkara et al., 2013) employed in previous studies. The photolysis frequency of NO_2, j_{NO2}, was measured to be 1.8×10^{-4} s^{-1} inside the reactor by a j_{NO2} filter radiometer (Meteorologie Consult, Germany), and it was smaller than the ground level j_{NO2} observed in surburban Hong Kong (with peaks at (3.0-6.0) $\times 10^{-3}$ sec^{-1}) (Xu et al., 2015). The lower light intensity was chosen to inhibit significant photolysis of NO_2 during the experiments and also represent the reduced light condition shaded by the high buildings in the city (Yun et al., 2017). Urban grime samples were collected by placing 20 cm × 10 cm glass plates underneath a building overhang at the Hong Kong Polytechnic University from August 21 to September 3, 2017, and the weight of each sample is about 0.01 g. A glass plate with urban grime was placed in the box reactor to investigate NO_2 uptake on urban grime or a clean glass plate was placed in the blank experiment. NO_2 and zero air were introduced in the box reactor and the total flow rate was changed from 3 to 5 L/min resulting in resistant time from 37.5 to 22.5 sec. The initial NO_2 concentration was 57 ppbv. A water bubbler was used to humidify the zero air and adjust

the RH. Photolysis experiments of urban grime were also tested, and the experiment setup and conditions were the same as the urban grime experiments except that only zero air was introduced into the reactor. The NO, NO_2 and HONO concentrations and RH were measured at the exit of the box reactor.

1.4 Instrumentation

At the exits of the reactors, NO and NO_2 concentrations were measured by a chemiluminescence analyzer with a photolytic converter (42i, Thermo Scientific, USA), HONO concentration was measured by a long-path absorption photometer (LOPAP, QUMA Elektronik & Analytik GmbH, Germany) (Heland et al., 2001; Xu et al., 2015) and the relative humidity (RH) was measured by a RH sensor (RH-USB, Omega, USA). Reacted and fresh urban grime samples were sonicated in 50 mL Milli-Q water to extract the inorganic compositions and the concentrations of the inorganic ions in the urban grime samples were measured by ion chromatography (ICS 1000, Dionex, USA).

1.5 Calculation of uptake coefficient

The reaction of NO_2 on different surfaces was assumed to be a pseudo-first-order reaction and the first-order rate constant (k_{obs}) can be calculated by:

$$k_{obs}=\ln\left(\frac{(NO_2)_0}{(NO_2)_t}\right)/t \quad (1)$$

where $(NO_2)_0$ (ppbv) is the initial NO_2 concentration and $(NO_2)_t$ (ppbv) is the NO_2 concentration after the reaction time t with the surface.

The geometric uptake coefficient γ_{geo} of the flow tube experiments can be calculated by:

$$\gamma_{geo}=\frac{2\,r_{tube}\,k_{obs}}{c} \quad (2)$$

where r_{tube} (m) is the radius of the flow tube and c (m/sec) is the average molecular velocity of NO_2.

The Cooney–Kim–Davis (CKD) method was used to correct the gas phase diffusion limitations in the calculation of the geometric uptake coefficient γ (Cooney et al., 1974; Murphy et al., 1987). And for the coated wall flow tube experiments, the true uptake coefficient (γ_{BET}) on particles was calculated by Eq. (3) (Underwood et al., 2000; Ma et al., 2017).

$$\gamma_{BET}=\frac{S_{geo}}{S_{BET}}\times\text{slope} \quad (3)$$

where S_{geo} (m^2) is the inner wall surface area of the quartz tube, S_{BET} (m^2) is the particle sample surface area and slope is the slope of the plot of the geometric uptake coefficient γ versus the sample mass in the linear regime.

The geometric uptake coefficient γ_{geo} in the urban grime experiments was calculated by:

$$\gamma_{geo}=\frac{4\,V_{box}\,(k_{obs\_grime}-k_{obs\_glass})}{S_{glass}\,c} \quad (4)$$

where k_{obs_grime} and k_{obs_glass} are the first-order rate constants measured with the urban grime sample or with a clean glass plate, the V_{box} (m^3) is the volume of the box reactor, S_{glass} (m^2) is the surface area of the glass plate and c (m/sec) is the average molecular velocity of NO_2.

Yields of NOHO and NO are calculated by:

$$\text{Yield}=\frac{(\Delta\text{Product})_{grime}-(\Delta\text{Product})_{glass}}{(\Delta NO_2)_{grime}-(\Delta NO_2)_{glass}} \quad (5)$$

where $(\Delta\text{Product})_{grime}$ (ppbv) and $(\Delta\text{Product})_{glass}$ (ppbv) are the HONO or NO concentrations produced from NO_2 reactions on urban grime or on a clean glass plate; $(\Delta NO_2)_{grime}$ (ppbv) and $(\Delta NO_2)_{glass}$ (ppbv) are the NO_2 consumed on urban grime or on a clean glass plate.

The flux of HONO production from the urban grime surface was calculated by:

$$\text{Flux}=\frac{((\Delta HONO)_{grime}-(\Delta HONO)_{glass})fP}{RTAS_{glass}} \quad (6)$$

where $(\Delta HONO)_{grime}$ (ppbv) and $(\Delta HONO)_{glass}$ (ppbv) are the HONO concentration produced from NO_2 uptake on urban grime of on a clean glass plate; f (m^3/sec) is the total flow introduced into the box reactor; P (Pa) is ambient pressure; R is molar gas constant, taken as 8.314 J/(mol·K); T (K) is ambient temperature; A is the Avogadro's constant; and S_{glass} (m^2) is the surface area of the glass plate.

2 Results and discussion

2.1 NO_2 uptake on inorganic particles

Fig. 2 shows the typical uptake experiment of NO_2 on inorganic particles, and the measured true uptake coefficient γ_{BET} on all of the tested inorganic particles are less than 3.2×10^{-7}, as summarized in **Table 1**. On each type of particles, experiments were conducted at least at two RH conditions. The results indicate that the heterogeneous uptake of NO_2 on these inorganic particles are generally weak, even at high humidity. In **Table 1**, previous results from other studies on inorganic particles are also summarized and compared (Underwood et al., 1999, 2001; Ndour et al., 2009; Borensen et al., 2000; Li et al., 2010b; Abbatt and Waschewsky, 1998; Harrison et al., 1998). The pressure and humidity conditions of the coated wall flow tube are much closer to ambient conditions than some techniques such as Knudsen cell reactor used in

the previous studies. The results measured in the present study are slightly higher than previous studies on the inorganic and mineral particle surfaces (Underwood et al., 1999, 2001; Ndour et al., 2009; Borensen et al., 2000; Li et al., 2010b; Zhou et al., 2015), except for NaCl (Abbatt and Waschewsky, 1998; Harrison et al., 1998). The γ_{BET} on NaCl was much smaller than the values measured in two previous studies using aerosol flow tube (10^{-4} to 10^{-3}) (Abbatt and Waschewsky, 1998; Harrison et al., 1998).

Several modeling studies adopted this higher value to estimate the HONO production from this heterogeneous process (Qiu et al., 2019; Alexander et al., 2020). However, our results suggest that the γ_{NO2} on NaCl particles are comparable to other inorganic particles. The discrepancy could be partially due to the different experimental techniques and also the much higher NO_2 concentration (ppmV level) in the previous studies.

Moreover, photo-enhanced uptake of NO_2 had been observed on mineral and soot particles because of the photocatalytic effects of TiO_2 and enhanced reactivity of NO_2 with PAH and other components (Ndour et al., 2008; Ndour et al., 2009; Al-Abadleh et al., 2000; Guan et al., 2017; George et al., 2015), while few experiments performed on inorganic particles under irradiation suggested an increased uptake but with much smaller effects than those on mineral and soot particles (Guan et al., 2014). In addition, a few studies have shown that multi-components in the particle play significant roles in the heterogeneous uptake of NO_2 and further nitrite formation (Tan et al., 2016; 2017). To address the unresolved daytime HONO source and the contributions from heterogeneous reaction on particles, further experiments under atmospheric conditions are still needed to measure the γ of NO_2 on multi-components system and real mixed ambient particles.

2.2 NO_2 uptake on sea water

As discussed before, the sea surface was suggested to be a potential source of HONO during nighttime (Zha et al., 2014), thus we used the wetted wall flow tube to investigate the NO_2 uptake on 3.5 wt.% NaCl solution and sea water. **Fig. 3** shows the example result of the NO_2 uptake experiment on sea water. It was surprising to find that HONO production was observed in the flow tube system when NO_2 had not contacted with the sea water surface (step 1). The background HONO was probably produced on the wall of the path tubing. However, when the extractor was pulled down and the NO_2 contacted with the sea water, both concentrations of NO_2 and HONO decreased (step 2-4). And when the contact of the NO_2 with the sea water was stopped, the NO_2 and HONO concentrations returned back to the initial concentrations (step 5). The γ_{geo} of NO_2 on NaCl solution and sea water was then calculated to be 1.4×10^{-8} and $1.6 \times$

10^{-8}, respectively (**Table 1**). These results suggest that the NO_2 uptake on sea water might not be a significant pathway to release gaseous HONO. The p*K*a of HONO is 3.4, and the pH of seawater in Hong Kong was reported to be 7.8-8.4 (Ning et al., 2006);thus alkaline conditions of sea water could retain the formed acidic HONO in the aqueous phase. Our results cannot help explain the elevated NO_2-to-HONO conversion rate in the nighttime air masses passing by sea surfaces observed by Zha et al. (2014). Another possible reason could be that the sea water used in the present study was the bulk water, while at the air−sea interface, there is a sea-surface microlayer (SML) comprised of complex enriched organic matters (Donaldson et al., 2012; Wurl and Obbard, 2004), which might be able to promote the heterogeneous conversion of NO_2 to HONO. In addition, several field measurements have observed daytime elevated HONO levels in the marine boundary layer, which were attributed to the photolysis of sea-salt nitrate or other nitrogen-containing compounds in SML (Kasibhatla et al., 2018; Wen et al., 2019). Due to the limitation of our experimental system, the irradiated experiment with sea water was not performed. Further experiments with the sea-surface microlayer under both dark and light conditions are still needed to better quantify the NO_2 heterogeneous process and understand the HONO formation in marine boundary layer.

2.3 NO_2 uptake on urban grime

Fig. 4 shows the steps of one experimental cycle to determine NO_2 uptake on urban grime. First, NO_2 was not introduced into the box reactor but passed through a bypass line until the NO_2 initial concentration was stable (step 1). Then NO_2 was introduced into the box reactor with the UV-visible light off (step 2). When the concentration of HONO and NO_2 were stable, the light was turned on and NO_2 uptake remained constant as long as the light was on (step 3). After that, the light was turned off (step 4) and NO_2 was bypassed from the box reactor (step 5). When the urban grime was exposed to NO_2 in the dark condition, NO_2 concentration decreased slightly (step 2 and 4), corresponding to an uptake coefficient below 3.1×10^{-7}. When the light was turned on, there was an obvious decrease of NO_2 compared to dark conditions, and the NO_2 uptake was constant during the irradiation (step 3). It suggests a weak uptake and reaction of NO_2 on urban grime in the dark condition, but an enhanced reaction under irradiation. The γ_{geo} on urban grime under irradiation was measured to be 1.9×10^{-6} at 5% RH and 5.8×10^{-6} at 70% RH, which shows a clear relative humidity dependence and is similar to the values of (1.1-5.8) $\times 10^{-6}$ at RH 0% - 90% reported by Liu et al. (2019).

Photo-enhanced uptake of NO_2 has also been found on polycyclic aromatic hydrocarbons (PAHs) (George et al., 2005; Brigante et al., 2008; Ammar et al., 2010; Cazoir et al., 2014), soot (Monge et al., 2010; Guan et al., 2016) and mineral dust (Ndour et al., 2008, 2009). PAHs

were proposed as photosensitizers to get excited under irradiation and react with NO_2, thus promote the NO_2 uptake (Monge et al., 2010). Ndour et al. (2008) found that TiO_2 can act as a photocatalyst and enhance the reactivity of NO_2 on mineral dust under irradiation. The true uptake coefficient (γ_{BET}) measured on soot and mineral dust in previous studies was calculated by measuring BET surface area of particle samples, and thus it may not be comparable to the geometric uptake coefficient on urban grime in the present study. Nevertheless, the γ_{geo} values of $(1.8 \pm 0.3) \times 10^{-6}$ on pyrene/KNO_3 under irradiation at 30%-35% RH (Ammar et al., 2010) are lower than the γ_{geo} on urban grime, which have more complex compositions than the proxies used in previous studies. In addition, Baltrusaitis et al. (2009) found that NO_2 uptake was enhanced on α-Fe_2O_3 surface under UV irradiation with reduced nitrogen species found on the surface. Mineral species like Fe, which has been found in urban grime (Lam et al., 2005), along with the mixture of PAHs, soot, TiO_2 and other photocatalysts in the urban grime, could significantly contribute to the photo-reactivity of urban grime and promote the NO_2-to-HONO conversion.

Formation of HONO and NO were also observed from the NO_2 uptake reactions on urban grime. When urban grime was exposed to NO_2 in the dark condition (cf. step 2 and step 4 in **Fig. 4**), the heterogeneous reaction of NO_2 only produced ~0.22 ppbv of HONO. At step 3, when urban grime was exposed to NO_2 under irradiation, enhanced formations of HONO (~0.86 ppbv) and NO (0.79 ppbv) were both observed. Nanayakkara et al. (2014) has shown that the photolysis of nitrate can contribute to HONO formation, so a photolysis experiment without NO_2 input was also carried out in the present study to assess the contribution from nitrate. Photolysis of nitrate in urban grime only contributed to ~0.20 ppbv of HONO.Compared with the ~0.86 ppbv HONO formed with the presence of NO_2, the photolysis of nitrate species in urban grime do contribute but only a small part of HONO formation. The heterogeneous reaction of NO_2 on urban grime is a dominant and more important source of HONO production in the urban area. There was no NO formation during the photolysis experiment, which indicated that NO formation was not due to the photolysis of HONO (figure not shown here). Furthermore, based on the measured photolysis frequency of NO_2 (j_{NO2}, 1.8×10^{-4} sec^{-1}), the photolysis only contributed to a loss of 0.7% of the total NO_2, suggesting that the formation of NO via NO_2 photolysis was also neglected in the present study. Similar to the present study, both formations of HONO and NO have been observed on illuminated PAHs and soot, and were attributed to the photosensitized reactions of NO_2 with PAHs (George et al., 2005; Brigante et al., 2008; Ammar et al., 2010; Cazoir et al., 2014; Monge et al., 2010). The observed HONO and NO could be contributed from the photo-reduction of NO_2 with PAHs or soot in urban grime.

However, only HONO formation was observed during the illuminated uptake of NO_2 on urban grime collected in Guangzhou (Liu et al., 2019), which may suggest the different reactions undergo on the surface of urban grime with different compositions. More experiments under different conditions with urban grime collected from different locations are still needed to better understand the NO_2 uptake and reactions on urban grime. Furthermore, the inorganic ions in the reacted and fresh urban grime was also compared in the present study (**Fig. 5**), and the mass fraction of nitrate in urban grime increased after exposure to NO_2 under irradiation. This indicated that the heterogeneous NO_2 uptake on urban grime also produced particulate nitrate besides the reduced gas-phase products.

The yields of NO and HONO on urban grime were calculated from the ratio of the net formation of NO or HONO to the net consumption of NO_2 by Eq. (5). The HONO yield was estimated to be 28% at 5% RH and 46% at 70% RH, and the NO yield was estimated to be 16% at 5% RH and 11% at 70% RH under irradiation. The positive correlations of NO_2 uptake and HONO formation with RH, indicating that high RH could enhance the uptake reaction. The amount of adsorbed water on urban grime has been found positively related to RH (Baergen and Donaldson, 2016). The adsorbed water could enhance the uptake by increasing the mobility of reagents (Rubasinghege and Grassian, 2013; Li et al., 2017) or reducing the viscosity of the surface (Renbaum-Wolff et al., 2013). Such changes in the mobility of reagents and viscosity of the surface could promote the reaction of NO_2 and the release of volatile products.

2.4 Atmospheric implication on HONO unknown source

The photo-enhanced HONO formation via NO_2 uptake could influence the oxidation capacity of the urban atmosphere, as an important source of OH radicals (e.g. Elshorbany, 2009). The flux of HONO production under irradiation can be calculated from the experiments, and it was determined to be 1.9×10^9 molecules/(cm^2·sec) at 5% RH and 5.3×10^9 molecules/(cm^2·sec) at 70% RH. Given in an urban area with 57 ppbv of NO_2 in a 10 m width street and 20 m height building covered with urban grime, an estimation of HONO source strength from urban grime using the geometric uptake coefficient could give 0.25 ppbv/hr at 5% RH and 0.71 ppbv/hr at 70% RH. Tang et al. (2015) found that there were high daytime missing sources of HONO in Beijing-Tianjin-Heibei region in China and the missing sources reached a maximum of 2.5 ppbV/hr. Lee et al. (2016) also reported the missing daytime source of HONO maximum of ~2.8 ppbV/hr in London. Accordingly, in a highly urbanized area, urban surfaces covered by urban grime such as buildings and roads provide a large surface area, and the NO_2 uptake on

the urban grime could be an important source of HONO in the daytime, and should be considered in the simulation of HONO levels in future modeling studies.

In view of the unknown HONO sources observed in different places, many air quality models have incorporated the NO_2 uptake process to better simulating the atmospheric HONO loading, which is of vital importance in assessing the oxidation capacity of the lower troposphere in polluted regions. In some model studies, larger γ was applied to better match the simulated HONO levels to measurements (Zhang et al., 2016, 2019, 2020). Nighttime uptake coefficients of 5×10^{-6} and 1×10^{-5} on the aerosol surface were used by Zhang et al. (2019) and Zhang et al. (2020), respectively, following the model setup in Li et al. (2010a). Yet, the uptake coefficient in Li et al. (2010a) was set as 1×10^{-6} according to a laboratory experiment for the NO_2 uptake on pure water and acidic solution (Kleffmann et al., 1998). Zhang et al. (2016) adopted a large uptake coefficient of 2×10^{-5} on the aerosol surface when sunlight was available, while the uptake coefficients reported by the references there ranged from 1.2×10^{-7} to 6×10^{-6} (George et al., 2005; Monge et al., 2010; Ndour et al., 2008; Stemmler et al., 2006). The Community Multiscale Air Quality (CMAQ) model adopted the γ_{geo} of 1×10^{-6} measured on tunnel wall by Kurtenbach et al. (2001) to simulate the heterogeneous formation of HONO on urban, leaves, and particle surfaces (Binkowski and Roselle, 2003; Byun and Schere, 2006; Foley et al., 2010). However, the real surface of the porous residue on the tunnel wall was not taken into consideration in γ_{geo}, and thus the true uptake coefficient on the residue particles should be smaller than the measured γ_{geo} (Kurtenbach et al., 2001), which should be only suitable for geometric surfaces such as ground and building surfaces. Besides, several model studies also used the γ_{geo} measured by Kurtenbach et al. (2001) as the γ_{BET} on particles (Vogel et al., 2003; Sarwar et al., 2008; Czader et al., 2012). Instead, the true uptake coefficient on particles such as γ_{BET} or γ measured in aerosol flow tube with directly measured particle surface area should be used in such cases. In most air quality models, a constant surface to volume ratio is usually used to estimate the building surface area in a given urban space, regardless of the ruggedness of the building surface (Zhang et al., 2016). The geometric uptake coefficient on urban grime does not consider the ruggedness of the grime surface either, and can be directly integrated into such air quality models. Inappropriate usages of γ of NO_2 in air quality models could lead to misestimates of HONO (Zhou et al., 2015). Therefore, more direct measurements of γ of NO_2 with real ambient aerosol and urban grime with mixture composition are needed. The uptake of NO_2 on different surfaces with different γ values also should be separately treated in the air quality models.

3 Conclusions

Heterogeneous uptake of NO_2 on different surfaces is an important process in controlling the NO_x removal from the atmosphere, and accurate representation of the NO_2 uptake coefficient in air quality models is of paramount importance for predicting the atmospheric NO_x cycling and photochemistry. In the present study, we measured the NO_2 uptake on different surfaces, including inorganic particles, sea water, and urban grime, using three different flow reactors, of which the experimental conditions are more close to ambient conditions. The reactivity of NO_2 was found very weak in dark conditions on such surfaces. The results showed that simple inorganic particles do not play an effective role in nighttime NO_2 heterogeneous uptake and HONO formation at ambient conditions, and further studies should be performed with multi-components system and complex real ambient particles. The bulk seawater can act as a nighttime sink of HONO, and additional efforts should be made to evaluate the role of the sea-surface microlayer (SML) on HONO formation in the marine boundary layer. More notably, UV-visible illumination enhanced the NO_2 uptake on urban grime by two orders of magnitude. HONO and NO formations were observed from the photo-enhanced NO_2 uptake on urban grime. The flux of HONO production from irradiated urban grime was determined to be (1.9-5.3) × 10^9 molecules/(cm^2·sec) at RH of 5% to 70%, which could lead to a daytime HONO source of 0.25-0.71 ppbv/hr in a presumptive urban street. The photo-enhanced NO_2 uptake on urban grime could increase the daytime HONO levels in the polluted urban atmosphere, and should be considered in future experimental and modeling studies.

Acknowledgments

This work was supported by the National Natural Science Foundation of China (Nos. 91844301, 91744204), and ANR-RGC Joint Research Scheme (project A-PolyU502/16-SEAM), and the Research Grants Council of Hong Kong Special Administrative Region, China (Nos. T24/504/17, 15265516, C5022-14G) and. We thank Dr. Tommy Wei for his help in the measurement of spectral irradiance of the UV-visible light.

References

Abbatt, J., Waschewsky, G., 1998. Heterogeneous interactions of HOBr, HNO_3, O_3, and NO_2 with deliquescent NaCl aerosols at room temperature. J. Phys. Chem. A 102, 3719-3725.

Al-Abadleh, H.A., Grassian, V.H., 2000. Heterogeneous reaction of NO_2 on hexane soot: A Knudsen cell and FT-IR study. J. Phys. Chem. A 104, 11926-11933.

Alexander, B., Sherwen, T., Holmes, C.D., Fisher, J.A., Chen, Q., Evans, M.J., et al., 2020. Global inorganic nitrate production mechanisms: comparison of a global model with nitrate isotope observations. Atmos. Chem. Phys. 20, 3859-3877.

Ammar, R., Monge, M.E., George, C., D'Anna, B., 2010. Photoenhanced NO_2 loss on simulated urban grime. Chemphyschem. 11, 3956-3961.

Angelini, M.M., Garrard, R.J., Rosen, S.J., Hinrichs, R.Z., 2007. Heterogeneous reactions of gaseous HNO_3 and NO_2 on the clay minerals maolinite and pyrophyllite. J. Phys. Chem. A 111, 3326-3335.

Baergen, A.M., Donaldson, D.J., 2013. Photochemical renoxification of nitric acid on real urban grime. Environ. Sci. Technol. 47, 815-820.

Baergen, A.M., Styler, S.A., van Pinxteren, D., Muller, K., Herrmann, H., Donaldson, D.J., 2015. Chemistry of urban grime: inorganic ion composition of grime vs particles in Leipzig, Germany. Environ. Sci. Technol. 49, 12688-12696.

Baltrusaitis, J., Jayaweera, P.M., Grassian, V.H., 2009. XPS study of nitrogen dioxide adsorption on metal oxide particle surfaces under different environmental conditions. Phys. Chem. Chem. Phys. 11, 8295-8305.

Behnke, W., George, C., Scheer, V., Zetzsch, C., 1997. Production and decay of $ClNO_2$ from the reaction of gaseous N_2O_5 with NaCl solution: Bulk and aerosol experiments. J. Geophys. Res. Atmos. 102, 3795-3804.

Binkowski, F.S., Roselle, S.J., 2003. Models-3 Community Multiscale Air Quality (CMAQ) model aerosol component 1. Model description. J. Geophys. Res. Atmos. 108, 4183.

Börensen, C., Kirchner, U., Scheer, V., Vogt, R., Zellner, R., 2000. Mechanism and kinetics of the reactions of NO_2 or HNO_3 with alumina as a mineral dust model compound. J. Phys. Chem. A 104, 5036-5045.

Brigante, M., Cazoir, D., D'Anna, B., George, C., Donaldson, D.J., 2008. Photoenhanced uptake of NO_2 by pyrene solid films. J. Phys. Chem. A 112, 9503-9508.

Butt, C.M., Diamond, M.L., Truong, J., Ikonomou, M.G., Ter Schure, A.F., 2004. Spatial distribution of polybrominated diphenyl ethers in southern Ontario as measured in indoor and outdoor window organic films. Environ. Sci. Technol. 38, 724-731.

Byun, D., Schere, K.L., 2006. Review of the governing equations, computational algorithms, and other components of the Models-3 Community Multiscale Air Quality (CMAQ) modeling system. Appl. Mech. Rev. 59, 51-76.

Cazoir, D., Brigante, M., Ammar, R., D'Anna, B., George, C., 2014. Heterogeneous photochemistry of gaseous NO_2 on solid fluoranthene films: a source of gaseous nitrous acid (HONO) in the urban environment. J. Photochem. Photobiol. A 273, 23-28.

Cooney, D.O., Kim, S.S., Davis, E.J., 1974. Analyses of mass transfer in hemodialyzers for laminar blood flow and homogeneous dialysate. Chem. Eng. Sci. 29, 1731-1738.

Czader, B.H., Rappenglück, B., Percell, P., Byun, D.W., Ngan, F., Kim, S., 2012. Modeling nitrous acid and its impact on ozone and hydroxyl radical during the Texas Air Quality Study 2006. Atmos. Chem. Phys. 12, 6939-6951.

Donaldson, D.J., George, C., 2012. Sea-surface chemistry and its impact on the marine boundary layer. Environ. Sci. Technol. 46, 10385-10389.

Elshorbany, Y.F., Kurtenbach, R., Wiesen, P., Lissi, E., Rubio, M., Villena, G., et al., 2009. Oxidation capacity of the city air of Santiago, Chile. Atmos. Chem. Phys. 9, 2257-2273.

Finlayson-Pitts, B.J., Wingen, L.M., Sumner, A.L., Syomin, D., Ramazan, K.A., 2003. The heterogeneous hydrolysis of NO_2 in laboratory systems and in outdoor and indoor atmospheres: An integrated mechanism. Phys. Chem. Chem. Phys. 5, 223-242.

Foley, K.M., Roselle, S.J., Appel, K.W., Bhave, P.V., Pleim, J.E., Otte, T.L., et al., 2010. Incremental testing of the Community Multiscale Air Quality (CMAQ) modeling system version 4.7. Geosci. Model Dev. 3, 205-226.

George, C., Strekowski, R.S., Kleffmann, J., Stemmler, K., Ammann, M., 2005. Photoenhanced uptake of gaseous NO_2 on solid-organic compounds: a photochemical source of HONO? Faraday Discuss. 130, 195-210.

George, C., Ammann, M., D'Anna, B., Donaldson, D.J., Nizkorodov, S.A., 2015. Heterogeneous photochemistry in the atmosphere. Chem. Rev. 115, 4218-4258.

Guan, C., Li, X., Luo, Y., Huang, Z., 2014. Heterogeneous Reaction of NO_2 on α -Al_2O_3 in the Dark and Simulated Sunlight. J. Phys. Chem. A 118, 6999-7006.

Guan, C., Li, X., Zhang, W., Huang, Z., 2017. Identification of nitration products during heterogeneous reaction of NO_2 on soot in the dark and under simulated sunlight. J. Phys. Chem. A 121, 482-492.

Gutzwiller, L., Arens, F., Baltensperger, U., Gaggeler, H.W., Ammann, M., 2002. Significance of semivolatile diesel exhaust organics for secondary HONO formation. Environ. Sci. Technol. 36, 677-682.

Han, C., Liu, Y., He, H., 2013. Role of organic carbon in heterogeneous reaction of NO_2 with soot. Environ. Sci. Technol. 47, 3174-3181.

Han, C., Yang, W., Wu, Q., Yang, H., Xue, X., 2016. Heterogeneous photochemical conversion of NO_2 to HONO on the humic acid surface under simulated sunlight. Environ. Sci. Technol. 50, 5017-5023.

Harrison, R.M., Collins, G.M., 1998. Measurements of reaction coefficients of NO_2 and HONO on aerosol particles. J Atmos. Chem. 30, 397-406.

Heland, J., Kleffmann, J., Kurtenbach, R., Wiesen, P., 2001. A new instrument to measure gaseous nitrous acid (HONO) in the atmosphere. Environ. Sci. Technol. 35, 3207-3212.

Kasibhatla, P., Sherwen, T., Evans, M.J., Carpenter, L.J., Reed, C., Alexander, B., et al., 2018. Global impact of nitrate photolysis in sea-salt aerosol on NOx, OH, and O_3 in the marine boundary layer. Atmos. Chem. Phys. 18, 11185-11203.

Kleffmann, J., Becker, K.H., Wiesen, P., 1998. Heterogeneous NO_2 conversion processes on acid surfaces: possible atmospheric implications. Atmos. Environ. 32, 2721-2729.

Kleffmann, J., 2007. Daytime sources of nitrous acid (HONO) in the atmospheric boundary layer. Chemphyschem. 8, 1137-1144.

Kurtenbach, R., Becker, K.H., Gomes, J.A.G., Kleffmann, J., Lorzer, J.C., Spittler, M., et al., 2001. Investigations of emissions and heterogeneous formation of HONO in a road traffic tunnel. Atmos. Environ. 35, 3385-3394.

Lam, B., Diamond, M.L., Simpson, A.J., Makar, P.A., Truong, J., Hernandez-Martinez, N.A., 2005. Chemical composition of surface films on glass windows and implications for atmospheric chemistry. Atmos. Environ. 39, 6578-6586.

Laufs, S., Kleffmann, J., 2016. Investigations on HONO formation from photolysis of adsorbed HNO_3 on quartz glass surfaces. Phys. Chem. Chem. Phys. 18, 9616-9625.

Lee, J.D., Whalley, L.K., Heard, D.E., Stone, D., Dunmore, R.E., Hamilton, J.F., et al., 2016. Detailed budget analysis of HONO in central London reveals a missing daytime source. Atmos. Chem. Phys. 16, 2747-2764.

Li, G., Lei, W., Zavala, M., Volkamer, R., Dusanter, S., Stevens, P., et al., 2010a. Impacts of HONO sources on the photochemistry in Mexico City during the MCMA-2006/MILAGO Campaign. Atmos. Chem. Phys. 10, 6551-6567.

Li, H.J., Zhu, T., Zhao, D.F., Zhang, Z.F., Chen, Z.M., 2010b. Kinetics and mechanisms of heterogeneous reaction of NO_2 on $CaCO_3$ surfaces under dry and wet conditions. Atmos. Chem. Phys. 10, 463-474.

Li, Y.J., Liu, P.F., Bergoend, C., Bateman, A.P., Martin, S.T., 2017. Rebounding hygroscopic inorganic aerosol particles: liquids, gels, and hydrates, Aerosol Sci. Technol. 51, 388-396.

Liang, Y., Zha, Q., Wang, W., Cui, L., Lui, K.H., Ho, K.F., et al., 2017. Revisiting nitrous acid (HONO) emission from on-road vehicles: a tunnel study with a mixed fleet. JAPCA. J. Air Waste Ma. 67, 797-805.

Liu, J., Li, S., Mekic, M., Jiang, H., Zhou, W., Loisel, G., et al., 2019. Photoenhanced uptake of NO_2 and HONO formation on real urban grime. Environ. Sci. Technol. Lett. 6, 413-417.

Liu, Q.T., Chen, R., McCarry, B.E., Diamond, M.L., Bahavar, B., 2003. Characterization of polar organic compounds in the organic film on indoor and outdoor glass windows. Environ. Sci. Technol. 37, 2340-2349.

Liu, Y., Han, C., Ma, J., Bao, X., He, H., 2015. Influence of relative humidity on heterogeneous kinetics of NO_2 on kaolin and hematite. Phys. Chem. Chem. Phys. 17, 19424-19431.

Ma, Q., Wang, T., Liu, C., He, H., Wang, Z., Wang, W., et al., 2017. SO_2 Initiates the efficient conversion of NO_2 to HONO on MgO surface. Environ. Sci. Technol. 51 ,3767-3775.

Monge, M.E., D'Anna, B., Mazri, L., Giroir-Fendler, A., Ammann, M., Donaldson, D.J., et al., 2010. Light changes the atmospheric reactivity of soot. P. Natl. Acad. Sci. USA. 107, 6605-6609.

Murphy, D.M., Fahey, D.W., 1987. Mathematical treatment of the wall loss of a trace species in denuder and catalytic converter tubes. Anal. Chem. 59, 2753-2759.

Nanayakkara, C.E., Jayaweera, P.M., Rubasinghege, G., Baltrusaitis, J., Grassian, V.H., 2014. Surface photochemistry of adsorbed nitrate: the role of adsorbed water in the formation of reduced nitrogen species on alpha-Fe_2O_3 particle surfaces. J. Phys. Chem. A 118, 158-166.

Ndour, M., D'Anna, B., George, C., Ka, O., Balkanski, Y., Kleffmann, J., et al., 2008. Photoenhanced uptake of NO_2 on mineral dust: laboratory experiments and model simulations. Geophys. Res. Lett. 35, L05812.

Ndour, M., Nicolas, M., D'Anna, B., Ka, O., George, C., 2009. Photoreactivity of NO2 on mineral dusts originating from different locations of the Sahara desert. Phys. Chem. Chem. Phys. 11, 1312-1319.

Ning, X., Chai, F., Hao, Q., 2006. Hypereutrophication in Ngau Mei Hoi Bay, Hong Kong. J. Coastal Res. 22, 1565-1572.

Qiu, X., Ying, Q., Wang, S., Duan, L., Zhao, J., Xing, J., et al., 2019. Modeling the impact of heterogeneous reactions of chlorine on summertime nitrate formation in Beijing, China. Atmos. Chem. Phys. 19, 6737-6747.

Renbaum-Wolff, L., Grayson, J.W., Bateman, A.P., Kuwata, M., Sellier, M., Murray, B.J., et al., 2013. Viscosity of α-pinene secondary organic material and implications for particle growth and reactivity. P. Natl. Acad. Sci. USA. 110, 8014-8019.

Rubasinghege, G., Grassian, V.H., 2013. Role(s) of adsorbed water in the surface chemistry of environmental interfaces. Chem. Commun. 49, 3071-3394.

Sarwar, G., Roselle, S.J., Mathur, R., Appel, W., Dennis, R.L., Vogel, B., 2008. A comparison of CMAQ HONO predictions with observations from the Northeast Oxidant and Particle Study. Atmos. Environ. 42, 5760-5770.

Stemmler, K., Ammann, M., Donders, C., Kleffmann, J., George, C., 2006. Photosensitized reduction of nitrogen dioxide on humic acid as a source of nitrous acid. Nature 440, 195-198.

Stemmler, K., Ndour, M., Elshorbany, Y., Kleffmann, J., D'anna, B., George, C., et al., 2007. Light induced conversion of nitrogen dioxide into nitrous acid on submicron humic acid aerosol. Atmos. Chem. Phys. 7, 4237-4248.

Su, H., Cheng, Y., Oswald, R., Behrendt, T., Trebs, I., Meixner, F.X., et al., 2011. Soil nitrite as a source of atmospheric HONO and OH radicals. Science 333, 1616-1618.

Tan, F., Jing, B., Tong, S., Ge, M., 2017. The effects of coexisting Na_2SO_4 on heterogeneous uptake of NO_2 on $CaCO_3$ particles at various RHs. Sci. Total Environ. 586, 930-938.

Tan, F., Tong, S., Jing, B., Hou, S., Liu, Q., Li, K., et al., 2016. Heterogeneous reactions of NO_2 with $CaCO_3$-$(NH_4)_2SO_4$ mixtures at different relative humidities. Atmos. Chem. Phys. 16, 8081-8093.

Tang, Y., An, J., Wang, F., Li, Y., Qu, Y., Chen, Y., et al., 2015. Impacts of an unknown daytime HONO source on the mixing ratio and budget of HONO, and hydroxyl, hydroperoxyl, and organic peroxy radicals, in the coastal regions of China. Atmos. Chem. Phys. 15, 9381-9398.

Underwood, G., Li, P., Usher, C., Grassian, V., 2000. Determining accurate kinetic parameters of potentially important heterogeneous atmospheric reactions on solid particle surfaces with a Knudsen cell reactor. J. Phys. Chem. A 104, 819-829.

Underwood, G., Miller, T., Grassian, V., 1999. Transmission FT-IR and Knudsen cell study of the heterogeneous reactivity of gaseous nitrogen dioxide on mineral oxide particles. J. Phys. Chem. A 103, 6184-6190.

Underwood, G., Song, C., Phadnis, M., Carmichael, G., Grassian, V., 2001. Heterogeneous reactions of NO_2 and HNO_3 on oxides and mineral dust: a combined laboratory and modeling study. J. Geophys. Res. Atmos. 106, 18055-18066.

Vogel, B., Vogel, H., Kleffmann, J., Kurtenbach, R., 2003. Measured and simulated vertical profiles of nitrous acid—Part II. Model simulations and indications for a photolytic source. Atmos. Environ. 37, 2957-2966.

599 Wang, L., Wang, W., Ge, M., 2012. Heterogeneous uptake of NO_2 on soils under variable
600 temperature and relative humidity conditions, J. Environ. Sci. 24, 1759-1766.
601 Wen, L., Chen, T., Zheng, P., Wu, L., Wang, X., Mellouki, A., et al., 2019. Nitrous acid in
602 marine boundary layer over eastern Bohai Sea, China: characteristics, sources, and
603 implications. Sci. Total Environ. 670, 282-291.
604 Wurl, O., Obbard, J.P., 2004. A review of pollutants in the sea-surface microlayer (SML): a
605 unique habitat for marine organisms. Mar. Pollut. Bull. 48, 1016-1030.
606 Xu, Z., Wang, T., Wu, J., Xue, L., Chan, J., Zha, Q., et al., 2015. Nitrous acid (HONO) in a
607 polluted subtropical atmosphere: seasonal variability, direct vehicle emissions and
608 heterogeneous production at ground surface. Atmos. Environ. 106, 100-109.
609 Ye, C., Gao, H., Zhang, N., Zhou, X., 2016. Photolysis of nitric acid and nitrate on natural and
610 artificial surfaces. Environ. Sci. Technol. 50, 3530-3536.
611 Ye, C., Zhang, N., Gao, H., Zhou, X., 2017. Photolysis of particulate nitrate as a source of
612 HONO and NO_x. Environ. Sci. Technol. 51, 6849-6856.
613 Yun, H., Wang, Z., Zha, Q., Wang, W., Xue, L., Zhang, L., et al., 2017. Nitrous acid in a street
614 canyon environment: sources and contributions to local oxidation capacity. Atmos.
615 Environ. 167, 223-234.
616 Zha, Q., Xue, L., Wang, T., Xu, Z., Yeung, C., Louie, P.K.K., et al., 2014. Large conversion
617 rates of NO_2 to HNO_2 observed in air masses from the South China Sea: evidence of strong
618 production at sea surface? Geophys. Res. Lett. 41, 7710-7715.
619 Zhang, J., An, J., Qu, Y., Liu, X., Chen, Y., 2019. Impacts of potential HONO sources on the
620 concentrations of oxidants and secondary organic aerosols in the Beijing-Tianjin-Hebei
621 region of China. Sci. Total Environ. 647, 836-852.
622 Zhang, J., Guo, Y., Qu, Y., Chen, Y., Yu, R., Xue, C., et al., 2020. Effect of potential HONO
623 sources on peroxyacetyl nitrate (PAN) formation in eastern China in winter. J. Environ.
624 Sci. 94, 81-87.
625 Zhang, L., Wang, T., Zhang, Q., Zheng, J., Xu, Z., Lv, M., 2016. Potential sources of nitrous
626 acid (HONO) and their impacts on ozone: a WRF-Chem study in a polluted subtropical
627 region. J. Geophys. Res. Atmos. 121, 3645-3662.
628 Zhou, L., Wang, W., Hou, S., Tong, S., Ge, M., 2015. Heterogeneous uptake of nitrogen dioxide
629 on Chinese mineral dust, J. Environ. Sci. 38, 110-118.
630 Zhou, X., Gao, H., He, Y., Huang, G., Bertman, S.B., Civerolo, K., et al., 2003. Nitric acid
631 photolysis on surfaces in low-NO_x environments: significant atmospheric implications.
632 Geophys. Res. Lett. 30, 2217.

633 **List of tables**

634 **Table 1** Summary of the NO_2 uptake coefficient (γ) on different surfaces

Surface	Irradiation	RH (%)	γ in this study	γ in previous studies	Experimental set-up in previous studies	References
SiO_2	Dark	10	$<10^{-8}$	$<10^{-10}$	At dry and vacuum condition; Knudsen cell reactor	Underwood et al., 2001
				$<10^{-9}$	At RH 25% and normal pressure; coated wall flow tube	Ndour et al., 2009
		85	$<10^{-8}$	-	-	-
Al_2O_3	Dark	7	3.2×10^{-8}	2×10^{-8}	At dry and vacuum condition; Knudsen cell reactor	Underwood et al., 1999
				1.3×10^{-9}-2.6×10^{-8}	At dry and vacuum condition; Diffuse Reflectance Infrared Fourier Transform Spectroscopy (DRIFTS)	Börensen et al., 2000
				1.20×10^{-9}	At dry and vacuum condition; DRIFTS	Guan et al., 2014
		80	1.4×10^{-8}	-	-	-
	Irradiated	-	-	3.33×10^{-9}	At dry and vacuum condition; DRIFTS	Guan et al., 2014
NaCl	Dark	5	$<10^{-8}$	-	-	-
		85	$<10^{-8}$	$<10^{-4}$	At RH 75% and normal pressure; aerosol flow tube	Abbatt and Waschewsky, 1998
				$(2.8\pm0.5) \times 10^{-4}$	At RH 85% and normal pressure; aerosol flow tube	Harrison and Collins, 1998
$CaCO_3$	Dark	10	2.5×10^{-7}	$(4.25\pm1.18) \times 10^{-9}$, $(3.34\pm0.14) \times 10^{-9}$	At dry and vacuum condition; DRIFTS	Li et al., 2010b
					At dry and vacuum condition; DRIFTS	Tan et al., 2016

		32	1.8×10^{-7}	$(2.04\pm0.07) \times 10^{-9}$	At RH 40% and vacuum condition; DRIFTS	Tan et al., 2016
		85	3.2×10^{-7}	$(6.56\pm0.34) \times 10^{-8}$ $(2.28\pm0.17) \times 10^{-9}$	At wet and vacuum condition; DRIFTS At RH 85% and vacuum condition; DRIFTS	Li et al., 2010b Tan et al., 2016
$(NH_4)_2SO_4$	Dark	10	$<10^{-8}$	$(3.19\pm0.21) \times 10^{-9}$- $(14.4\pm1.07) \times 10^{-9}$	$(NH_4)_2SO_4$-$CaCO_3$ mixture, at dry and vacuum condition; DRIFTS	Tan et al., 2016
		56	$<10^{-8}$	$(2.25\pm0.14) \times 10^{-9}$- $(12.7\pm0.81) \times 10^{-9}$	$(NH_4)_2SO_4$-$CaCO_3$ mixture, at RH 60% and vacuum condition; DRIFTS	Tan et al., 2016
		85	$<10^{-8}$	$(2.00\pm0.21) \times 10^{-9}$- $(7.48\pm0.82) \times 10^{-9}$	$(NH_4)_2SO_4$-$CaCO_3$ mixture, at RH 85% and vacuum condition; DRIFTS	Tan et al., 2016
Mineral dust	Dark	-	-	8.0×10^{-8}- 2.3×10^{-7}	At dry and vacuum condition; DRIFTS	Angelini et al., 2007
				10^{-9}	At RH 25% and normal pressure; coated wall flow tube	Ndour et al., 2008
	Irradiated	-	-	1.2×10^{-7}- 1.9×10^{-6}	At RH 25% and normal pressure; coated wall flow tube	Ndour et al., 2008
Soot	Dark	-	-	4.72×10^{-5} (initial) 0.74×10^{-5} (140 sec average)	At dry and vacuum condition; Knudsen cell reactor	Al-Abadleh et al., 2000

				1.46×10^{-5} (initial) 0.85×10^{-5} (15 min average)	At RH 32% and normal pressure; coated wall flow tube	Guan et al., 2017
	Irradiated	-	-	1.60×10^{-5} (initial) 1.02×10^{-5} (15 min average)	At RH 32% and normal pressure; coated wall flow tube	Guan et al., 2017
3.5 wt.% NaCl solution	Dark	-	1.4×10^{-8}	-	-	-
Bulk sea water	Dark	-	1.6×10^{-8}	-	-	-
Urban grime	Dark	5 70	$<10^{-7}$ 3.1×10^{-7}	-	-	-
	Irradiated	5	1.9×10^{-6}	$(1.1 \pm 0.2) \times 10^{-6}$	At RH 0% and normal pressure; coated wall flow tube	Liu et al., 2019
		70	5.8×10^{-6}	$(5.8 \pm 0.7) \times 10^{-6}$	At RH 90% and normal pressure; coated wall flow tube	Liu et al., 2019

635

636

List of figures

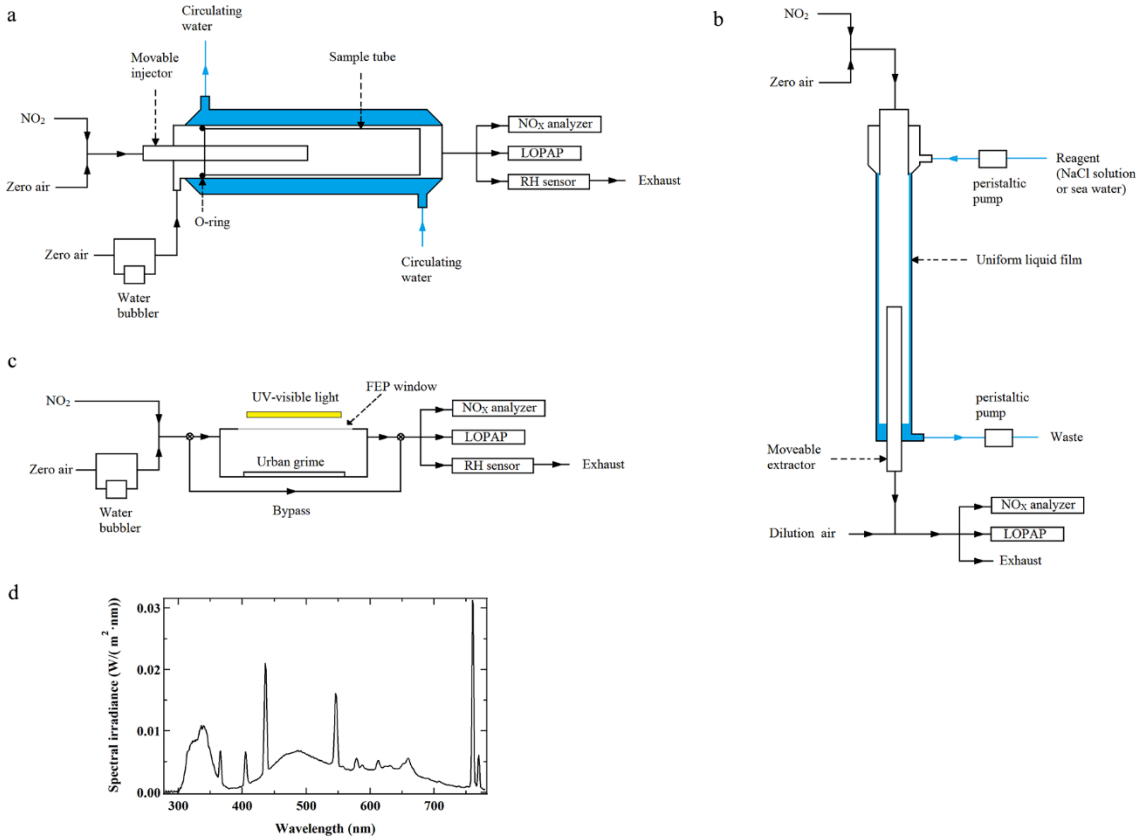

Fig. 1 Schematic diagrams of (a) the coated wall flow tube system, (b) the wetted wall flow tube system, and (c) the Teflon box reactor system. (d) Spectral irradiance of the UV-visible light measured in the Teflon reactor. LOPAP: long-path absorption photometer; RH: relative humidity.

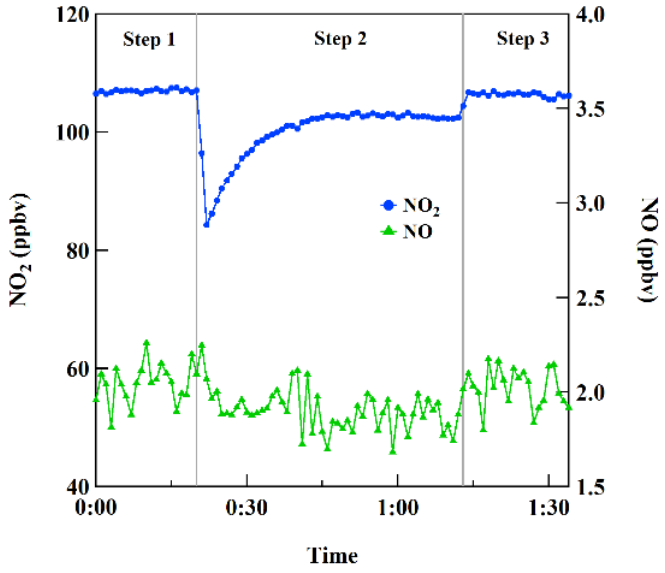

Fig. 2 NO_2 uptake on $CaCO_3$ at 32% RH. Blue circles and green triangles represent the NO_2, and NO concentrations at the exit of the reactor. The grey vertical lines indicate the experimental steps. Step 1: reactor bypass; step 2: $CaCO_3$ exposed to NO_2 in the dark; step 3: reactor bypass line.

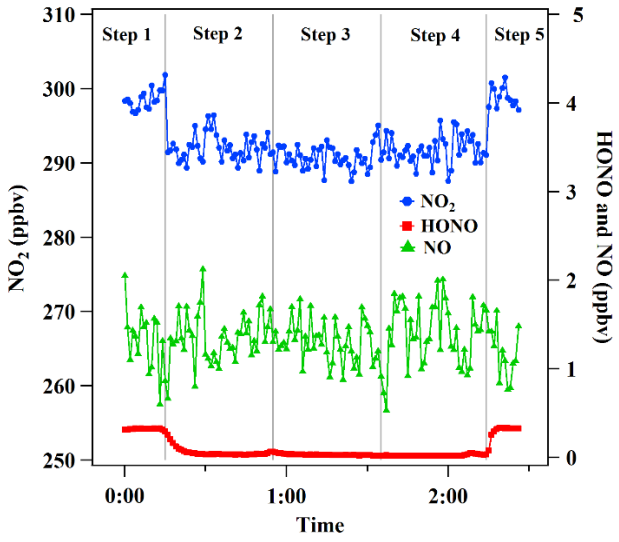

Fig. 3 NO_2 uptake on bulk sea water. RH measured at the exit of the flow tube was 26%. Blue circles, red squares and green triangles represent the NO_2, HONO and NO concentrations at the exit of the reactor. The grey vertical lines indicate the experimental steps. Step 1: the extractor was at top of the wetted wall flow tube, the gas-liquid contact distance l = 0 cm; step 2: pulling down the extractor, l = 10 cm; step 3: l = 20 cm; step 4: l = 30 cm; step 5: the extractor was pushed back to the top of the wetted wall flow tube, l = 0 cm. l: gas-liquid contact distance.

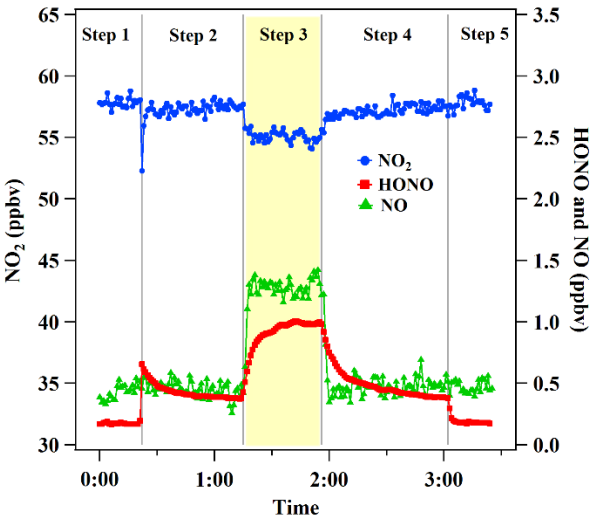

Fig. 4 Conversion of NO_2 to HONO and NO on urban grime at 70% RH. Blue circles, red squares and green triangles represent the NO_2, HONO, and NO concentrations at the exit of the reactor. The grey vertical lines indicate the experimental steps. Step 1: reactor bypass; step 2: urban grime exposed to NO_2 in the dark; step 3: urban grime exposed to NO_2 under the irradiation; step 4: urban grime exposed to NO_2 in the dark; step 5: reactor bypass.

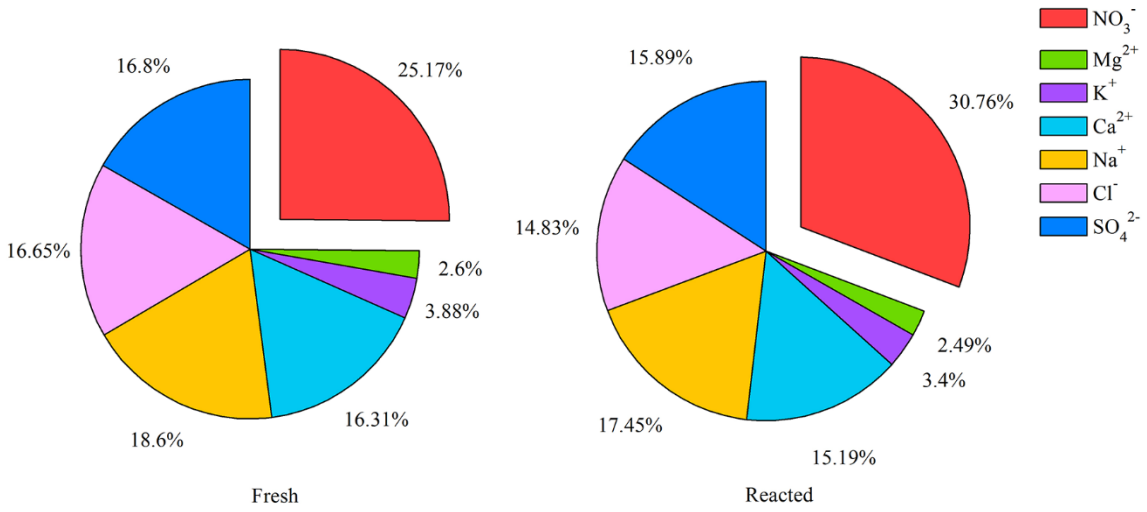

Fig. 5 Mass fractions of inorganic ions in the fresh urban grime and the reacted urban grime after the irradiation experiment.